2018 21st International Conference on Intelligent Transportation Systems (ITSC)
Maui, Hawaii, USA, November 4-7, 2018

Cooperative Adaptive Cruise Control in Vehicle Platoon under Environment of i-VICS

Jishiyu DING
Department of Automation
Tsinghua University
Beijing, China
djsy15@mails.tsinghua.edu.cn

Huaxin PEI
Department of Automation
Tsinghua University
Beijing, China
phx17@mails.tsinghua.edu.cn

Jianming HU
Department of Automation
Tsinghua University
Beijing, China
hujm@mail.tsinghua.edu.cn

Yi ZHANG*
Department of Automation, Beijing National Research Center (BNRist), Tsinghua University, Beijing, China
Tsinghua -- Berkeley Shenzhen Institute (TBSI), Nanshan Intelligence Park 1001, Shenzhen, China
zhyi@mail.tsinghua.edu.cn

***Abstract*—With the rapid development in vehicular communication technologies, driving assistance systems of intelligent vehicles can provide promising efficiency, safety and sustainability to the intelligent transportation systems. In this paper, a cooperative adaptive cruise control (CACC) approach is proposed for vehicle platoon under the environment of Intelligent Vehicle Infrastructure Cooperative Systems (i-VICS). The cooperative adaptive cruise control problem consists of three parts, the vehicle dynamics, longitudinal control and lateral control. Moreover, the packet loss ratio and time delay are taken into account in the simulation to investigate their impacts on the performance of CACC. Furthermore, some field tests are carried out with two autonomous vehicles to verify the effectiveness of the proposed method. According to the results of simulation and field tests, the proposed CACC approach shows great benefits on longitudinal and lateral control in vehicle platoon.**

Keywords—cooperative adaptive cruise control, vehicle platoon, i-VICS, packet loss ratio, time delay

I. INTRODUCTION

Vehicle control technologies are expected to yield manifold benefits in the transportation systems. On one hand, fully automated cooperative systems show significant improvement on the efficiency. On the other hand, autonomous driver-assistance systems are beneficial to enhance the driving safety, particularly with respect to rear-end collisions. Adaptive cruise control (ACC) is one of the popular driving assistance systems, which has been developed rapidly in recent years and can provide a safe and efficient driving environment for drivers in the Automated Highway System (AHS) [1]-[3].

With the development of communication technologies in the last decade, vehicle to vehicle (V2V) and vehicle to infrastructure (V2I) technologies show promising potential in intelligent transportation systems. Vehicles equipped with OBU can cooperate to provide a safe and efficient traffic environment based on information sharing. Thus, cooperative adaptive cruise control (CACC) in vehicle platoon has become a critical issue in the vehicle platooning problem.

Prior experimental results using vehicle-vehicle cooperation to improve vehicle-following performance were achieved by the California Partners for Advanced Transit and Highways (PATH) in 1997 [4]. When a platooning maneuver involving eight fully automated cars was carried out using wireless communication among vehicles, mainly for longitudinal control, and magnetic markers in the infrastructure, mainly for lateral control. Girard et al. [5] built a control architecture for integrated cooperative cruise control and collision warning systems, which separated the complex problem into several sub-problems and addressed in separate layers. Ploeg et al. [6] designed and evaluated a longitudinal cooperative adaptive cruise control to reduce the traffic congestion. In 2011, Desjardins et al. [7] utilized a reinforcement learning approach to achieve cooperative adaptive cruise control in the longitudinal following process, which can result in efficient behavior for CACC. Öncü et al. [8] proposed an analysis technique that can be used to investigate tradeoffs between CACC performance (string stability) and network specifications (such as delays), which are essential in the multidisciplinary design of CACC controllers. In 2010, Naus et al. [9] designed a cooperative adaptive cruise control system using wireless communication and achieved small inter-vehicle distances, while maintaining string stable behavior. Werf et al. [11] investigated the effects of adaptive cruise control systems on highway traffic flow capacity using Monte Carlo simulations. The results of this study can help to provide realistic estimates of the effects of the introduction of ACC to the vehicle fleet. According the previous studies on ACC and CACC, it can be found that those literatures mainly focused on the longitudinal control and most of them utilized simulation to verify the effectiveness of proposed method. Lateral control of CACC is usually ignored in the vehicle platoon. Moreover, some field tests with autonomous vehicles in the real world need to be done to evaluate the performance of CACC approach.

In this paper, a cooperative adaptive cruise control (CACC) approach for vehicle platoon is proposed, including longitudinal control and lateral control. Longitudinal control of CACC is responsible for the speed adjustment and distance adjustment, while lateral control is utilized to keep vehicle platoon during turning. Some simulation-based experiments are implemented to verify the effectiveness of the CACC approach. Moreover, packet loss ratio and time delay are taken into account to investigate their impacts on the performance of CACC. Furthermore, field tests with two autonomous vehicle are carried out to evaluate the performance of proposed method.

The remaining of the paper is organized as follows. Section II describes the cooperative adaptive cruise control approach. A simulation-based case study and corresponding results are presented in Section III. Moreover, some field tests are carried out in Section IV. Finally, concluding remarks are presented in Section V.

*Corresponding author. E-mail :zhyi@mail.tsinghua.edu.cn

II. COOPERATIVE ADAPTIVE CRUISE CONTROL APPROACH

A. Vehicle Dynamics

According to the previous studies [14]-[15], the vehicle dynamics can be described by Equation (1) and Equation (2). In this model, the vehicle is simplified to a bicycle model, which uses steering angle and acceleration (deceleration) as system inputs.

$$(k_1 + k_2)\beta + \frac{1}{u}(ak_1 - bk_2)\omega_r - k_1\delta = m(v + \dot{u}\omega_r) \quad (1)$$

$$(ak_1 - bk_2)\beta + \frac{1}{u}(a^2k_1 + b^2k_2)\omega_r - ak_1\delta = I_z\dot{\omega}_r \quad (2)$$

where a is the distance between the center of mass and the front tire, b is the distance between the center of mass and the rear tire, k_1 is the stiffness coefficient of the front tire, k_2 is the stiffness coefficient of the rear tire, ω_r is the yaw rate of the vehicle, β is the vehicle sideslip angle which is between the heading of the vehicle and the velocity of its center of mass, I_z is the moment of inertia around the vertical axis through center of mass, δ is the front steering angle.

Equation (1) and Equation (2) can be transformed into Equation (3) and Equation (4) with matrix forms. Furthermore, they can be simplified as Equation (5) and Equation (6).

$$\dot{\omega}_r = \frac{(a^2k_1 + b^2k_2)}{I_z u}\omega_r + \frac{(ak_1 - bk_2)}{I_z}\beta - \frac{ak_1}{I_z}\delta \quad (3)$$

$$\dot{\beta} = \left(\frac{(ak_1 - bk_2)}{mu^2} - 1\right)\omega_r + \frac{(k_1 + k_2)}{mu}\beta - \frac{k_1}{mu}\delta \quad (4)$$

$$\begin{bmatrix}\dot{\omega}_r \\ \dot{\beta}\end{bmatrix} = \begin{bmatrix}a_{11} & a_{12} \\ a_{21} & a_{22}\end{bmatrix}\begin{bmatrix}\omega_r \\ \beta\end{bmatrix} + \begin{bmatrix}b_{11} \\ b_{21}\end{bmatrix}\delta \quad (5)$$

$$\begin{bmatrix}\omega_r \\ \beta\end{bmatrix} = \begin{bmatrix}1 & 0 \\ 0 & 1\end{bmatrix}\begin{bmatrix}\omega_r \\ \beta\end{bmatrix} + \begin{bmatrix}0 \\ 0\end{bmatrix}\delta \quad (6)$$

$$\begin{aligned} x &= Ax + Bu \\ y &= Cx + Du \end{aligned} \quad (7)$$

where $a_{11} = \frac{(a^2k_1+b^2k_2)}{I_z u}$, $a_{12} = \frac{(ak_1-bk_2)}{I_z}$, $b_{11} = -\frac{ak_1}{I_z}$, $a_{21} = \frac{(ak_1-bk_2)}{mu^2} - 1$, $a_{22} = \frac{(k_1+k_2)}{mu}$ and $b_{21} = -\frac{k_1}{mu}$.

B. CACC Approach

Cooperative adaptive cruise control can be implemented by two separated parts: longitudinal control and lateral control. The vehicle speed is adjusted by the longitudinal control and the steering angle of vehicle is adjusted by the lateral control.

1) Longitudinal Control

The target of the longitudinal control is to achieve the desired speed and the desired distance between vehicles in the platoon. Therefore, this objective can be formulated as Equation (8).

$$\begin{cases}\lim\limits_{t\to\infty}\|v_i(t) - v_d(t)\| = 0 \\ \lim\limits_{t\to\infty}\|p_{i-1}(t) - p_i(t) - d_{i-1,i}\| = 0\end{cases}, i \in N \quad (8)$$

where $v_i(t)$ is the speed of the vehicle i at time t, $v_d(t)$ is the desired speed at time t, $p_{i-1}(t)$ is the position of vehicle $i-1$ at time t, $p_i(t)$ is the position of i_{th} vehicle at time t, $d_{i-1,i}$ is the desired distance between vehicle i and vehicle $i-1$ at time t, N is the number of vehicles in the platoon.

The desired distances in the vehicle platoon are assumed to be equal as described in Equation (9)-(10).

$$d_{i,i} = 0,\ d_{i,i-1} = -d_{i-1,i} \quad (9)$$

$$d_{i-1,i} = d_{i,des} \quad i \in N \quad (10)$$

PID controller is utilized in the longitudinal control process. Thus, the longitudinal control law is formulated as Equation (11).

$$\begin{aligned} v_i(t+1) = K_p * \big(p_i(t) - p_{i-1}(t) - i * d_{i,des}\big) \\ + K_v\big(v_{i-1}(t) - v_i(t)\big) + v_i(t) \end{aligned} \quad (11)$$

The performances of the longitudinal control are reflected by the control error of vehicle speed and vehicle distance:

$$\delta_i = p_{i-1}(t) - p_i(t) - d_{i-1,des} \quad (12)$$

where δ_i is the distance error between vehicle i and vehicle $i-1$.

$$\Delta v_i = v_{i-1} - v_i \quad (13)$$

where Δv_i is the speed error between vehicle i and vehicle $i-1$.

2) Lateral Control

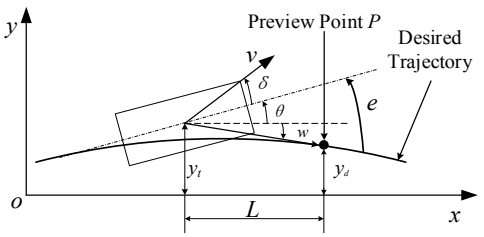

Fig. 1. Diagram of the lateral control model

A virtual preview point P is set in front of the vehicle as shown in Fig. 1. A PID controller is used to adjust the steering angle of the vehicle. The diagram of the lateral controller is shown in Fig. 2.

$$e(t) = \theta(t) - w(t) \quad (14)$$

$$w(t) = arctan\frac{y_t - y_d}{L} \quad (15)$$

where $e(t)$ is the error between actual heading angle and desired heading angle at time t, $\theta(t)$ is the heading angle of vehicle at time t, $w(t)$ is the desired heading angle, (x_t, y_t) is the position of vehicle at time t, (x_d, y_d) is the position of the preview point at time t, L is the preview distance.

$$\delta(t) = k_p * e(t) + \frac{1}{k_i} * \sum e(t) + k_d * \big(e(t) - e(t-1)\big) \quad (16)$$

where $\delta(t)$ is the steering angle of vehicle at time t, k_p is the coefficient of the proportional part, k_i is the coefficient of integral part, k_d is the coefficient of the differential part,

$e(t-1)$ is the error between actual heading angle and desired heading angle at time $t-1$.

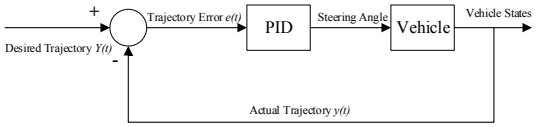

Fig. 2. Diagram of the lateral controller

C. Communication Model

1) Packet Loss Model

The packet loss model is based on the Bernoulli distribution, which is formulated as Equation (17):

$$P_r[\theta(k)=0]=p,\quad P_r[\theta(k)=1]=1-p \tag{17}$$

where $\theta(k)$ is a random Bernoulli process. $\theta(k)=0$ represents that packet loss occurs during the communication, while $\theta(k)=1$ means that there is no packet loss. Thus, p denotes the packet loss ratio.

DSRC and LTE-V are utilized in the experiments and their relationship between packet reception ratio and communication distance are shown in Fig. 3. The packet reception ratio decreases with the increase of communication distance.

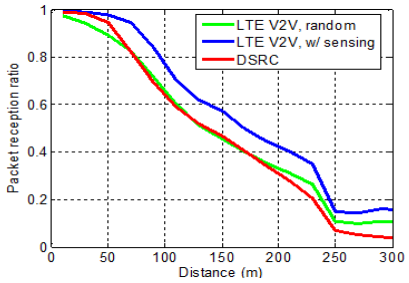

Fig. 3. Diagram of relationship between packet recepion ratio and distance

2) Time Delay Model

A time delay model is built to simulate the communication delay in the actual situations. The observation state is received as the real state with time delay t_{del} as Equation (18).

$$x_{obs}(t)=x_{real}(t-t_{del}) \tag{18}$$

where $x_{obs}(t)$ denotes the observation state at time t, $x_{real}(t)$ denotes the real state at time t, t_{del} represents the time delay.

On account of the communication delay, the PID controll law utilized in the longitudinal control should be modified as Equation (19).

$$\begin{aligned} v_i(t+1)=&K_p*\left(p_i(t)-p_0(t-t_{del})-i*d_{i,des}\right)\\ &+K_v\left(v_0(t-t_{del})-v_i(t)\right)+v_0(t-t_{del}) \end{aligned} \tag{19}$$

III. Simulation and Results

In this section, some simulation-based experiments are carried out with the consideration of the impacts of packet loss ratio and time delay.

A. Simulation Parameters

The simulation parameters of the vehicle dynamics are set as TABLE I. . The details of information exchange are shown in TABLE II. . TABLE III. shows the control variables of the autonomous vehicle.

TABLE I. Table of Parameter Setings

Variable	Definition	Value
m	The mass of vehicle	$1500kg$
I_z	The moment of inertia	$2500\ kg\cdot m^2$
a	The distance between the center of mass and the front tire	$1.20m$
b	The distance between the center of mass and the rear tire	$1.50m$
k_1	The stiffness coefficient of front tire	$80000\ N/rad$
k_2	The stiffness coefficient of rear tire	$80000\ N/rad$

TABLE II. Table of Information Exchange

Information Item	Unit
Longitude	°
Latitude	°
Speed	m/s
Acceleration	m/s^2

TABLE III. Table of Control Variables

Variable	Unit
Desired speed	m/s
Acceleration	m/s^2
Desired steering angle	°
Desired steering yaw rate	$°/s$

B. Results under Perfect Communication Conditions

The results under perfect communication conditions are shown in Fig. 4 to Fig. 6. The trajectory of following vehicle is perfectly fitting in with the trajectory of leading vehicle in Fig. 4. Furthermore, the trajectory error in Fig. 5 ranges from -0.17m to 0.17m. It can be found that the trajectory error increases while the curvature of the trajectory increases. Fig. 6 shows the steering angle of the following vehicle, which is relatively smooth in lateral control process.

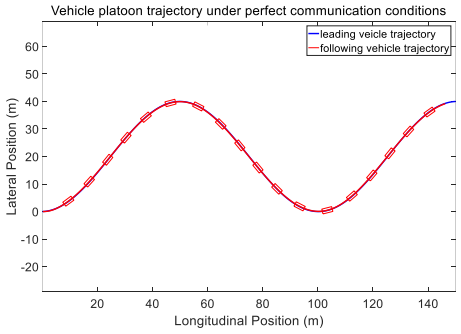

Fig. 4. Diagram of vehicle trajectory under perfect communication conditions

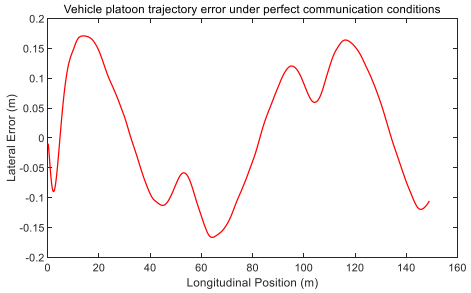

Fig. 5. Diagram of vehicle trajectory error under perfect communication conditions

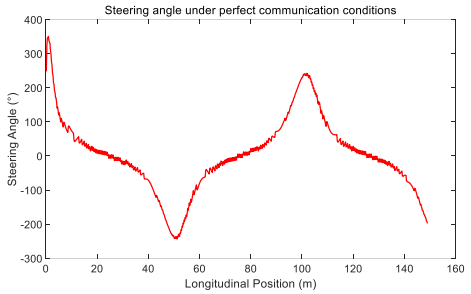

Fig. 6. Diagram of vehicle steering angle under perfect communication conditions

C. *Results under Imperfect Communication Conditions*

In the actual situation, communication condition may be not perfect, which means there are packet loss and time delay during the process of information exchange. Thus, the impacts of packet loss ratio and time delay on the lateral control error are further investigated.

1) Packet Loss Ratio

The packet loss ratio is set as 0.2, 0.4, 0.6, and 0.8, respectively. In each scenario, the vehicle trajectories and position error of lateral control are recorded.

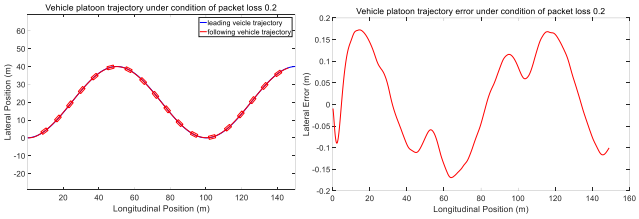

Fig. 7. Diagram of vehicle trajectory error under condition of packet loss ratio 0.2

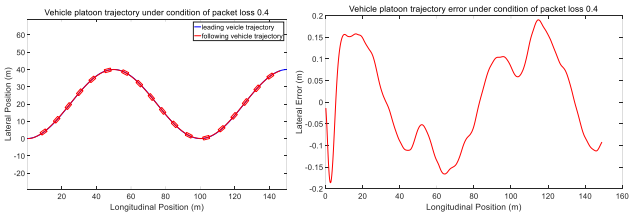

Fig. 8. Diagram of vehicle trajectory error under condition of packet loss ratio 0.4

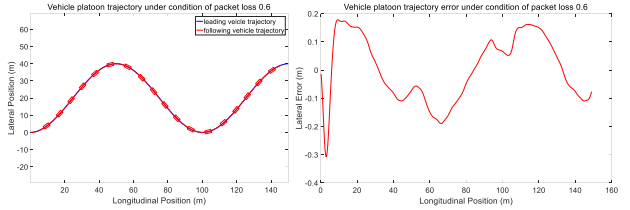

Fig. 9. Diagram of vehicle trajectory error under condition of packet loss ratio 0.6

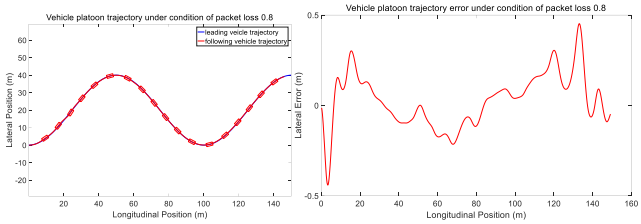

Fig. 10. Diagram of vehicle trajectory error under condition of packet loss ratio 0.8

From Fig. 7 to Fig. 10, we can find that the position error of lateral control increases with the increase of the packet loss ratio during the process of vehicle platoon control. The error threshold is set as $0.4m$. Therefore, the packet loss ratio should be less than 0.6 in the simulation experiments to meet the requirement.

Since the frequency of communication is set as $0.02s$, the following vehicle could get the packet per $0.1s$ theoretically even if the packet loss ratio reaches 0.8. Thus, the frequency of communication should be no less than $10Hz$ during the simulation.

2) Time Delay

The time delay is set as $0.05s$, $0.1s$, $0.15s$ and $0.2s$, respectively. In each scenario, the vehicle trajectories and position error of lateral control are recorded.

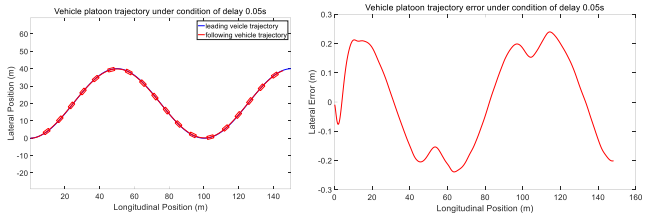

Fig. 11. Diagram of vehicle trajectory error under condition of time delay 0.05s

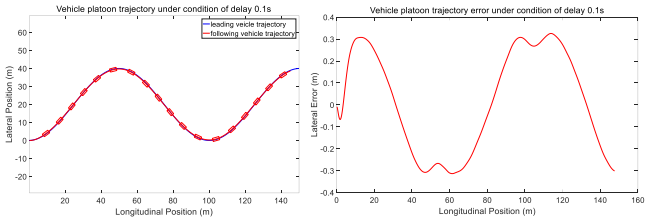

Fig. 12. Diagram of vehicle trajectory error under condition of time delay 0.1s

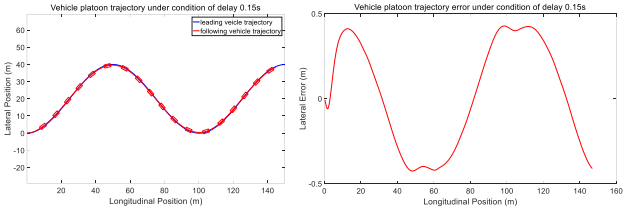

Fig. 13. Diagram of vehicle trajectory error under condition of time delay 0.15s

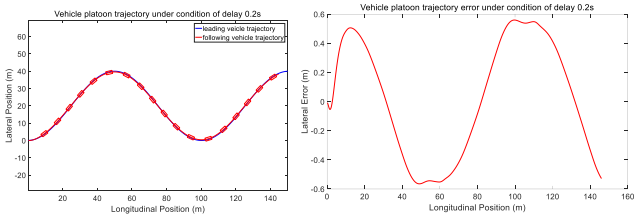

Fig. 14. Diagram of vehicle trajectory error under condition of time delay 0.2s

From Fig. 11 to Fig. 14, it can be found that the lateral control error increases with the increase of the time delay during the process of vehicle platoon control. The error threshold is set as $0.4m$. Therefore, the time delay should be less than $0.15s$ in the simulation experiments to meet the requirement.

IV. Field Tests and Results

Fig. 15. Diagram of CACC field tests

Field tests are carried out in the Shanghai International Automobile City in 2016. As shown in Fig. 15, two autonomous vehicle are utilized to form a vehicle platoon and completed the CACC tasks. The communication mode in this experiment is LTE-V. Both longitudinal and lateral control of CACC are tested in the test field and the result are as follows.

A. Longitudinal Control Results

In the real-world test, the time delay of communication is set as $10\,ms$, $100\,ms$ and $150\,ms$ respectively and the standard distance between vehicles is set as $10m$. The speed of vehicles and the distance between vehicles are recorded.

1) Time delay 10ms

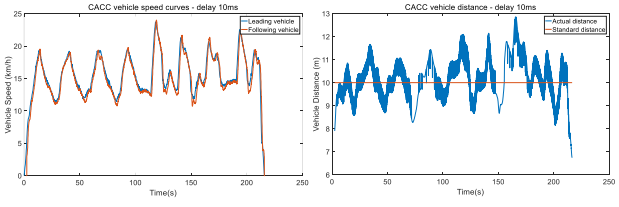

Fig. 16. Longitudinal control results under condition of time delay 10ms

From Fig. 16, it can be found that the speed curves of two vehicles are approximately overlapped. The speed of leading vehicle (the blue curve) ranges from $10km/h$ to $20km/h$ and the following vehicle can adjust its speed timely according to the leading vehicle. The distance between vehicle ranges from $8m$ to $12m$. The performance of longitudinal control of CACC is relatively good with time delay of $10ms$.

2) Time delay 100ms

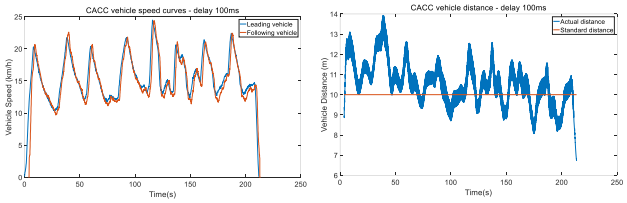

Fig. 17. Longitudinal control results under condition of time delay 100ms

From Fig. 17, it can be found that the speed curve of the following vehicle is slightly left behind the leading vehicle. Since the exist of $100ms$ time delay, the distance between two vehicles also increases. Even though, the two vehicles can complete the longitudinal car-following task tolerably.

3) Time delay 150ms

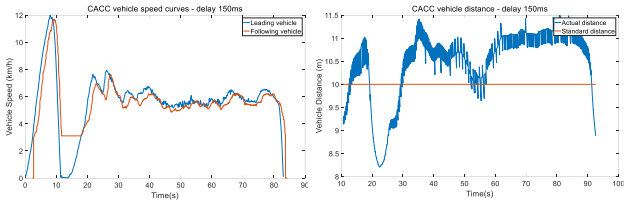

Fig. 18. Longitudinal control results under condition of time delay 150ms

When the time delay increases to $150ms$, a serious speed error occurs during the time $10s$ and $20s$. Therefore, the requirement of time delay less than $0.15s$ is verified further.

B. Lateral Control Results

The test field in the lateral control experiments is shown in Fig. 19, which consists of two U-turn and some straightaways. The vehicle trajectories and the steering angle are recorded to evaluate the performance of lateral control in the real-world tests.

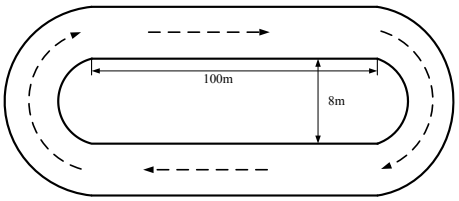

Fig. 19. Diagram of the test field in lateral control

The results of lateral control in test field is shown in Fig. 20. The blue curve denotes the trajectory of leading vehicle, while the red one denotes the trajectory of following vehicle. With the proposed CACC approach, the following vehicle

can follow the leading vehicle with small position error. After the statistics, the average position error is about $0.8m$ during the experiment. It is noted that this position error contains the error of GPS. According to the measure of GPS performance, the average position error of GPS range from $0.3m$ to $0.4m$ approximately. Therefore, the maximal control error of CACC approach ranges from $0.4m$ to $0.5m$.

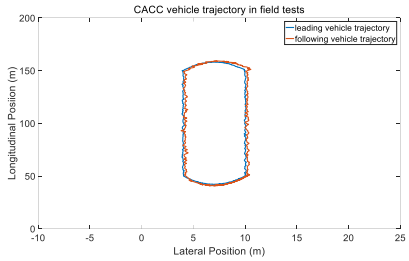

Fig. 20. Diagram of lateral control results

Furthermore, the steering angle of the following vehicle is shown in Fig. 21. The curve of steering angle is relatively smooth, which verify the effectiveness of the proposed CACC approach.

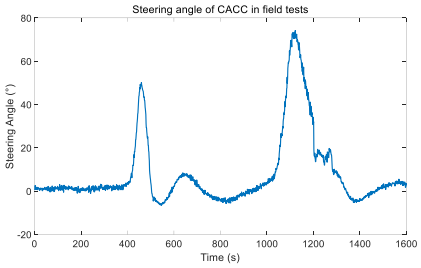

Fig. 21. Diagram of the steering angle in lateral control

V. CONCLUSION

In this paper, a cooperative adaptive cruise control (CACC) approach is proposed for vehicle platoon under the environment of I-VICS. With the V2V wireless communication, the proposed method can provide accurate and efficient longitudinal and lateral control during vehicle platooning. Based on simulation-based experiments, the proposed CACC approach can achieve trajectory following with position error less than $0.17\ m$ under perfect communication condition. Moreover, packet loss ratio and time delay are taken into account in the simulation to investigate their impacts on the performance of CACC. According to the simulation results, to achieve the performance of position error less than $0.4m$, packet loss ratio should no more than 0.6 and time delay should no more than $0.15s$ during vehicle platooning. Finally, some field tests are carried out with two autonomous vehicles in the Shanghai International Automobile City. The results show that the proposed CACC approach show great benefits on both longitudinal control and lateral control in vehicle platoon. Since we use U-turn as the scenario to verify the effectiveness of lateral control, the limitation of this work lies in the low velocity during the turning process. More field tests with high velocity will be carried out in the future work.

ACKNOWLEDGMENT

This work is supported by National Natural Science Foundation of China under Grant No. 61673233 and No. 61673232, Beijing Municipal Science and Technology Program under Grant D171100004917001/2 and D171100006417003 and National Key R&D Program in China (2016YFB0100906).

REFERENCES

[1] Vahidi, A., & Eskandarian, A. (2004). Research advances in intelligent collision avoidance and adaptive cruise control. *IEEE Transactions on Intelligent Transportation Systems, 4*(3), 143-153.

[2] Guvenc, L., Uygan, I. M. C., Kahraman, K., Karaahmetoglu, R., Altay, I., & Senturk, M., et al. (2012). Cooperative adaptive cruise control implementation of team mekar at the grand cooperative driving challenge. *IEEE Transactions on Intelligent Transportation Systems,13*(3), 1062-1074.

[3] Ioannou, P. /., & Chien, C. C. (1993). Autonomous intelligent cruise control. *IEEE Transactions on Vehicular Technology, 42*(4), 657-672.

[4] Shladover, S. E. (2007). PATH at 20—History and major milestones. *IEEE Transactions on intelligent transportation systems*, *8*(4), 584-592.

[5] Girard, A. R., Sousa, J. B. D., Misener, J. A., & Hedrick, J. K. (2002). A control architecture for integrated cooperative cruise control and collision warning systems. *Decision and Control, 2001. Proceedings of the, IEEE Conference on* (Vol.2, pp.1491-1496 vol.2). IEEE.

[6] Ploeg, J., Serrarens, A. F. A., & Heijenk, G. J. (2011). Connect & drive: design and evaluation of cooperative adaptive cruise control for congestion reduction. *Journal of Modern Transportation, 19*(3), 207-213.

[7] Desjardins, C., & Chaib-Draa, B. (2011). Cooperative adaptive cruise control: a reinforcement learning approach. *IEEE Transactions on Intelligent Transportation Systems, 12*(4), 1248-1260.

[8] Sinan Öncü, Ploeg, J., Wouw, N. V. D., & Nijmeijer, H. (2014). Cooperative adaptive cruise control: network-aware analysis of string stability. *IEEE Transactions on Intelligent Transportation Systems, 15*(4), 1527-1537.

[9] Naus, G., Vugts, R., Ploeg, J., & Van, d. M. R. (2009). Cooperative adaptive cruise control, design and experiments. *American Control Conference* (Vol.58, pp.6145-6150). IEEE.

[10] Bu, F., Tan, H. S., & Huang, J. (2010). Design and field testing of a Cooperative Adaptive Cruise Control system. *American Control Conference* (Vol.58, pp.4616-4621). IEEE.

[11] Werf, J. V., Shladover, S., Miller, M., & Kourjanskaia, N. (2002). Effects of adaptive cruise control systems on highway traffic flow capacity.*Transportation Research Record Journal of the Transportation Research Board, 1800*(1), 78-84.

[12] Milanes, V., Shladover, S. E., Spring, J., Nowakowski, C., Kawazoe, H., & Nakamura, M. (2014). Cooperative adaptive cruise control in real traffic situations. *IEEE Transactions on Intelligent Transportation Systems,15*(1), 296-305.

[13] Shladover, S. E., Nowakowski, C., Lu, X. Y., & Ferlis, R. (2016). Cooperative adaptive cruise control. *Transportation Research Record Journal of the Transportation Research Board, 2489*, 145-152.

[14] Li, L., Wang, F. Y., & Zhou, Q. (2006). Integrated longitudinal and lateral tire/road friction modeling and monitoring for vehicle motion control.*IEEE Transactions on Intelligent Transportation Systems, 7*(1), 1-19.

[15] Georg. (2011). *Road vehicle dynamics : fundamentals and modeling*. CRC Press.